THE ASTROPHYSICAL JOURNAL, 320:482–492, 1987 September 15

CCD PHOTOMETRY OF GLOBULAR CLUSTER CORE STRUCTURE. I. NGC 6388, NGC 6624, AND M15—ONE FLAT CORE AND TWO CUSPS

PHYLLIS M. LUGGER[1,2] AND HALDAN COHN[1,2]
Department of Astronomy, Indiana University

JONATHAN E. GRINDLAY[1] AND CHARLES D. BAILYN[2]
Department of Astronomy, Harvard University

AND

PAUL HERTZ
E.O. Hulbert Center for Space Research, Naval Research Laboratory
Received 1986 November 3; accepted 1987 February 9

ABSTRACT

We report the first results of a major survey of globular cluster core structure. We have obtained *UBVR* CCD frames of the cores of 72 globular clusters using the CTIO 4 m and KPNO No. 1 0.9 m telescopes. A principal goal of this work is to test the prediction that a significant number of Galactic globular clusters have undergone core collapse and should therefore have central surface brightness cusps. Such cusps have now been reported in 21 out of 123 clusters studied by Djorgovski and King. We present surface brightness profiles for three clusters: one with a normal flat core profile—NGC 6388—and two with central cusps—NGC 6624 and M15 (NGC 7078). A major advantage of our work is the use of *U*-band CCD data which produce better determined surface brightness profiles since cluster images are less dominated by small numbers of red giants in the *U* band than at longer wavelengths. We have fitted these profiles with both seeing-convolved King models and seeing-convolved power laws. A King model provides a reasonable fit to the entire profile of NGC 6388. In contrast, there are no acceptable King model fits to the entire profiles of NGC 6624 and M15. For these two clusters, a seeing-convolved power law provides a good fit to the inner part of the profile ($r < 10''$), while a King model gives a good fit to the outer part of the profile ($r > 10''$). We discuss the interpretation of the measured power-law slopes of the central surface brightness cusps of NGC 6624 and M15 in terms of models for core collapse in a multicomponent cluster.

Subject headings: clusters: globular — photometry — stars: stellar dynamics

I. INTRODUCTION

a) Theoretical Background

The inexorable evolution of dense stellar systems toward core collapse is now well established by detailed computer simulations (see Spitzer [1985] for a recent review). Core collapse is the process by which star-star gravitational scatterings drive the core radius of a globular cluster to very small values ($<10^{-2}$ pc), while the central density increases to extremely large values ($>10^8\ M_\odot\ \mathrm{pc}^{-3}$). For a typical globular cluster, the time to core collapse is less than the Hubble time. The analyses of the observed distribution of globular cluster central relaxation times by Lightman (1982) and Cohn and Hut (1984) suggest that as many as 25% of all Galactic globular clusters have already experienced core collapse. Twenty five years ago Hénon (1961) predicted that the observational signature of a cluster that has undergone core collapse is a central surface brightness cusp—a surface brightness profile that continues to rise as a power law at small radii in contrast to a normal King-type (1966*a*) profile that becomes flat within a core radius of the cluster center.[3] Detailed cluster evolution simulations by Larson (1970) and Cohn (1980) confirmed the predicted development of a cusp during core collapse. The expected slope of this cusp in a cluster containing identical stars (-1.2 in projection) was first accurately determined by Lynden-Bell and Eggleton (1980) and Cohn (1980). Subsequent investigations of cusp development, including the effects of velocity distribution anisotropy, close stellar encounters, and particle discreteness, have been carried out by Duncan and Shapiro (1982), Goodman (1983), and McMillan and Lightman (1985*a*, *b*), respectively. Inagaki and Saslaw (1985) and Murphy and Cohn (1987) have performed detailed simulations of the development of a cusp in a cluster containing a realistic stellar mass spectrum.

If the cusp that develops during core collapse is long-lived, a powerful observational test of the theory is possible. Under the dense conditions that result from core collapse, rates of binary formation by two-star tidal interactions and three-star interactions are substantially enhanced. The former mechanism is likely to be responsible for the production of X-ray binary systems in high central density clusters (Grindlay 1985). It is generally thought that cluster cores undergo a postcollapse expansion that is driven by energy release from hard binaries which interact with single stars and each other (Hut 1985). A question of fundamental importance to the prospects for observational tests of the theory is how long it takes the core to

[1] Visiting Astronomer, Cerro Tololo Inter-American Observatory, National Optical Astronomy Observatories, which is operated by the Association of Universities for Research in Astronomy, under contract with the National Science Foundation.

[2] Visiting Astronomer, Kitt Peak National Observatory. National Optical Astronomy Observatories, which is operated by the Association of Universities for Research in Astronomy, under contract with the National Science Foundation.

[3] The median value of the core radius for Galactic globular clusters is ~ 1 pc (Peterson 1976) which subtends an angle of 20″ at the Galactic center.

expand back to its resolvable precollapse size, possibly erasing the evidence that the cluster underwent core collapse. In the past few years an intensive effort has been undertaken by several research groups to develop good models for postcollapse clusters containing binaries (Inagaki and Lynden-Bell 1983; Sugimoto and Bettwieser 1983; Heggie 1984; Goodman 1984; Stodółkiewicz 1985; Ostriker 1985; Cohn 1985; McMillan 1986; Statler, Ostriker, and Cohn 1987; Lee 1987; Cohn, Hut, and Wise 1987). Many theoretical issues concerning binary-driven postcollapse evolution remain unresolved such as the stability of the cluster to core structure oscillations. However, the results of most of these studies indicate that the core radius remains unresolvable for at least 1–2 Gyr following core collapse and that the density profile has a power-law form in the region between the core and halo. Thus all studies predict that globular clusters that have undergone core collapse *recently* will have central surface brightness cusps at the present time.

In a cluster of identical stars, the slope of the surface brightness cusp immediately following core collapse is expected to be -1.2 (Cohn 1980). (By slope we mean $d \log S/d \log r$, where S is surface brightness measured in intensity units; for a King model, $d \log S/d \log r$ rapidly tends to zero inside the core radius.) Several studies predict a slope of -1.0 during the binary-driven postcollapse expansion phase (Inagaki and Lynden-Bell 1983; Heggie 1984; Goodman 1984; Statler, Ostriker, and Cohn 1987). However, for a realistic cluster mass spectrum, the expected slope of the cusp depends on the ratio of the mass of the red giants (that dominate the luminosity) to the mass of the nonluminous remnants (that dominate the gravitational potential). The smaller this ratio, the flatter the surface brightness cusp (Bahcall and Wolf 1977; Larson 1984; Cohn and Hut 1984; Cohn 1985). For a red giant mass of 0.7 $M_\odot$ and a maximum white dwarf mass of 1.0 $M_\odot$, the predicted slope around the time of core collapse is -0.7 (Cohn 1985). Accurate observational determinations of the slopes of cusps will constrain the cluster mass function.

b) *Previous and Concurrent Observational Work*

During the past several years there has been mounting observational evidence for the existence, in several globular clusters, of the central surface brightness cusps predicted by the theory of core collapse. The clusters M15 and NGC 6624 have received particular attention since these are among 10 clusters with high-luminosity ($>10^{36}$ ergs s^{-1}) X-ray sources (Grindlay 1985). The electronographic surface photometry of M15 reported by Newell and O'Neil (1978) provided the first strong evidence for the presence of a central cusp. This cusp in M15 is also detected by the photoelectric photometry of King (1966*b*), the photographic photometry of Cordoni and Aurière (1981) and Hertz and Grindlay (1985), and the CCD photometry of Djorgovski and Penner (1985) and Lugger, Cohn, and Grindlay (1985). Djorgovski and King (1984) and Hertz and Grindlay (1985) detected a cusp in NGC 6624 using photographic photometry that is confirmed by our CCD data (Lugger, Cohn, and Grindlay 1985). Djorgovski and King (1986) have been carrying out a large-scale survey of globular cluster core structure in parallel with our work. They have recently reported definite cusps in 21 clusters and possible cusps in seven others out of 123 clusters surveyed, mostly using CCD data in the *BVR* bands.

c) *The Present Study*

We report here on observations of three clusters: two showing central surface brightness cusps, NGC 6624 and M15, and for comparison a cluster which shows no evidence of a surface brightness cusp, NGC 6388. This latter cluster has been cited by Djorgovski and King (1986) as a prototype of their "normal" class of clusters with profiles that closely resemble standard King models. The profiles that we present from our U-band CCD photometry for these clusters are significantly better determined (i.e., smaller statistical errors) than previously published profiles for these clusters.

Visual inspection of U-band images of NGC 6624 and M15 indicates apparent surface brightness "spikes" about 2″–3″ in radius at the cluster centers. Our surface brightness profiles presented in § IV indicate that these spikes represent the central few arcsec of the power-law cusps that extend out to about 10″ in both clusters. When the surface brightness profiles are plotted in the usual log (surface brightness)–log (radius) plane, it is evident that what is perceived as a small-scale spike in the cluster image is in fact a smooth continuation of a larger radius power-law feature. We shall use the term "cusp" to describe the entire central power-law structure.

Section II of this paper describes our observational techniques. Section III presents our data analysis methods. We report our results in § IV and discuss these results in § V.

II. OBSERVATIONS

a) *Telescopes and Detectors*

We have used RCA CCD chips on the CTIO 4 m and KPNO No. 1 0.9 m telescopes for our survey. The greater throughput of the 4 m telescope is particularly useful for obtaining adequate signal-to-noise U-band exposures of reddened southern clusters. CCD detectors are ideally suited for this investigation because of their high quantum efficiency and wide dynamic range. The image scale is 0″.60 per pixel at prime focus on the 4 m and 0″.48 per pixel at the f/13.5 focus on the No. 1 0.9 m telescope, resulting in fields of approximately 3′ (N–S) × 5′ (E–W) for both telescopes. These pixel sizes adequately sample the seeing disk which is typically 1″.5 FWHM for our data. Recently, we have used the 3.6 m Canada-France-Hawaii telescope to carry out high angular resolution follow-up observations of several clusters that show strong evidence of central cusps.

b) *UBVR Photometry*

Our study has concentrated on obtaining U-band frames of globular cluster cores in addition to B, V, and R frames. Cluster images are less dominated by individual red giants in the U, and are thus less "noisy," than at longer wavelengths (King 1980, 1985; Hertz and Grindlay 1985). Thus U-band images produce smoother, better determined surface brightness profiles that are more representative of the underlying mass distribution. This is important for our study, since we want to determine slopes of surface brightness cusps with the highest possible accuracy. Our photometric system is defined by standard *UBVR* filter sets. The CTIO U filter used for most of our observations is an interference type while the KPNO U filter is a UG-2 with $CuSO_4$ red blocking. The peak transmissions for these filters are about 30% and 60%, respectively.

Exposure times are determined by the condition that we obtain the highest pixel signal-to-noise ratio possible without saturating the cores of bright stellar images. At CTIO we have generally been able to expose, in all filters but U, to the point where the Poisson noise in the sky is equal to the readout noise of the chip ($90e^-$ and $75e^-$ per pixel at CTIO and KPNO, respectively). Inordinately long exposures would be required to achieve this condition using the f/13.5 focus on the KPNO No.

1 0.9 m telescope. Thus at KPNO, we instead expose to the point where the sky exceeds the linearity threshold for the chip ($\sim 500e^-$). Most of the integration time is spent in the U filter at both telescopes, since the system throughput in U is down by factors of 10 and 5 relative to B for the CTIO and KPNO systems, respectively. U-band exposures are generally limited to 20 minutes at both telescopes, although exposures of several hours would be possible for some clusters without saturating the highest intensity pixel.

c) *The Cluster Sample*

We have generally restricted our sample to clusters with core radii of less than 0'.5 (using the compilation of Webbink [1985]) so that it is possible to determine the surface brightness profile out to 5 core radii for a cluster centered in the field. It is necessary to determine the profile to at least several core radii in order to accurately fit a King model. We also observed a number of clusters with larger core radii ($\sim 1'$) for comparison. The determination of cluster centers requires that the entire core be observed, so that 1' is about the largest core radius that can be handled using a single CCD field. For many of the clusters in our CTIO sample, we obtained an additional set of exposures with the cluster center offset from the center of the CCD frame by 2' to the east or west end of the frame. These offset exposures were generally done in BVR only. The offset frames allow the determination of profiles out to 10 core radii. To date we have obtained data for 72 clusters, with at least one complete set of $UBVR$ frames for most clusters. The most highly reddened clusters [$E(B-V) > 1.0$] were observed only in R or I or both, while some moderately reddened clusters [$0.5 < E(B-V) < 1.0$] were observed in BVR only.

d) *Observations of NGC 6388, NGC 6624, and M15*

As discussed in § Ic, we report here on observations of NGC 6388, NGC 6624, and M15. Some properties of these clusters, taken from Webbink's (1985) compilation, are listed in Table 1: R_0, the heliocentric distance; M_V, the total absolute visual magnitude; ρ_0, the central density; r_c, the core radius; and r_t, the tidal radius. The nominal central densities of these three clusters are almost identical and are at the upper end of the observed distribution. The nominal core radii are all below the median of the observed distribution. However, there is a marked difference in the central surface brightness profiles of NGC 6624 and M15 relative to that of NGC 6388.

Our present data base of CCD frames for these three clusters is as follows. NGC 6388 was observed once from CTIO in $UBVR$ (1985 May). NGC 6624 was observed twice from CTIO in $UBVR$ (1984 August and 1985 May) and once from KPNO in U and R (1984 May). M15 was observed twice from KPNO in $UBVR$ (1984 May and September). Deep U-band exposures were obtained for all three clusters. The surface brightness profiles that we report here were determined from frames taken in 1985 May for NGC 6388 and NGC 6624, and 1984 May for M15. Analysis of the stellar content of these and other clusters using our CCD frame data base will be reported separately.

TABLE 1

CLUSTER PROPERTIES

Cluster	R_0 (kpc)	M_V	$\log \rho_0\ (M_\odot\ \mathrm{pc}^{-3})$	r_c (pc)	r_t (pc)
NGC 6388	13.5	−9.91	5.27	0.58	32.6
NGC 6624	8.0	−7.46	5.32	0.20	26.8
M15 (NGC 7078) ...	9.7	−8.67	5.26	0.26	59.1

III. DATA ANALYSIS

a) *Surface Brightness Profile Determination*

We have determined cluster surface brightness profiles from our CCD frames using software kindly made available to us by S. Djorgovski and I. King. The procedure has been described by Djorgovski and King (1984) and Djorgovski (1987). The first step is to determine the center of maximum symmetry of the cluster using a mirror-autocorrelation method (see Fig. 2 of Djorgovski [1987]). This centering method is similar to that of Hertz and Grindlay (1985), who used one-dimensional autocorrelation sums to determine the X and Y coordinates of the cluster center separately.

Once the cluster center has been determined, the surface brightness profile is computed for a set of logarithmically spaced concentric circular annuli that are each divided into eight sectors. The location of the center of a pixel determines which annulus and sector it lies in. Surface brightness values are computed for each individual sector of an annulus. The error in the mean surface brightness value for the annulus is taken to be the standard deviation of the sector surface brightness values divided by the square root of the number of sectors. If a particular sector contains no pixel centers, it is not counted in the average. In principal, the distribution of the eight sector values of surface brightness can be used to study the azimuthal symmetry of these clusters. We will carry out such an analysis in future work.

The sky value for a frame is determined by computing the modes of the pixel intensity histograms for 50 pixel × 50 pixel windows in the four corners of the frame. The lowest of the four modes is taken as the best estimate of the sky since this usually corresponds to the window farthest from the cluster center. This procedure may somewhat overestimate the sky if there is a substantial diffuse component to the cluster surface brightness distribution. In any case, the determined sky values are about two orders of magnitude smaller than the central surface brightness and so the central part of the profile is not much affected by the adopted sky value.

b) *PSF Determination*

The point-spread function (PSF) is determined for each CCD frame by computing stellar profiles using software adapted from the University of California Santa Cruz VISTA system. The routine was originally developed by S. Kent for determining profiles of elliptical galaxies, but it is equally well suited to studying stellar profiles. We put the stellar profile into an axisymmetric form by expressing surface brightness as a function of isophote mean radius.

We are generally able to follow the profiles of relatively isolated bright stars to a radius of about 5" before encountering other fainter stars. We have used P. Stetson's DAOPHOT PSF routines for removing neighboring stars in the M15 U frame and find that this does not significantly alter the determined stellar profiles or the seeing-convolved model fits to the cluster profiles.

c) *Profile Fitting*

A central question we address in this study is: Are the seeing-deconvolved central surface brightness profiles of M15 and NGC 6624 pure power laws, as predicted by theory? We address this question by fitting seeing-convolved power-law models to the observed profiles since the data are not suffi-

1987ApJ...320..482L

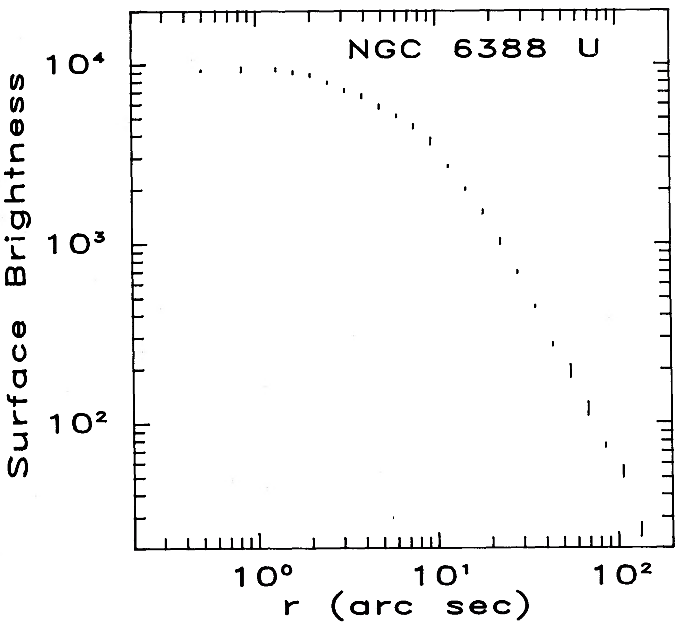

FIG. 1*a*

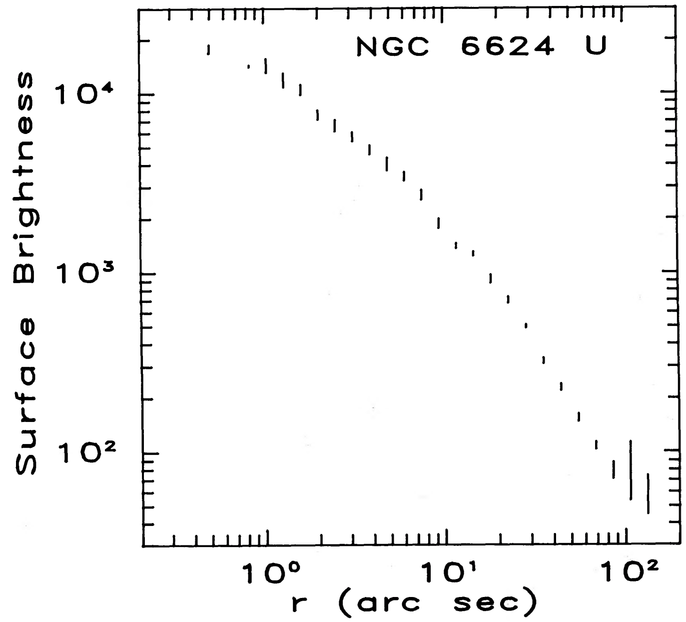

FIG. 1*b*

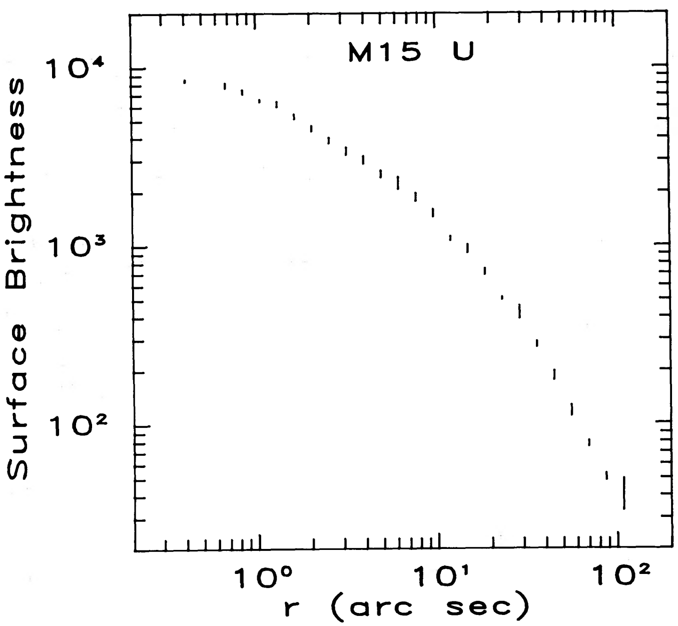

FIG. 1*c*

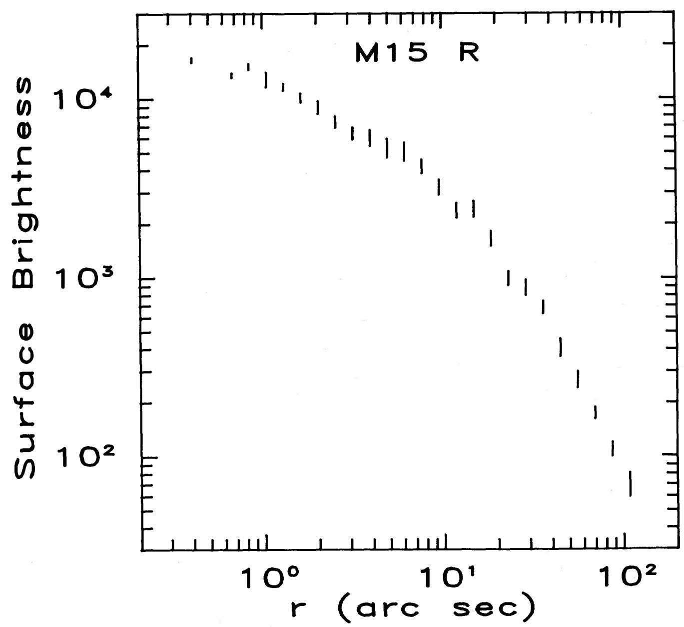

FIG. 1*d*

FIG. 1.—Surface brightness profiles of NGC 6388, NGC 6624, and M15. (*a*)–(*c*) are *U*-band profiles while (*d*) is an *R*-band profile of M15 for comparison. The profiles are uncalibrated and are expressed in terms of ADU per pixel, where 1 ADU corresponds to approximately 10 photoelectrons. Telescopes and exposure times are (*a*) CTIO 4 m, 600 s; (*b*) CTIO 4 m, 1200 s; (*c*) KPNO No. 1, 0.9 m, 1800 s; (*d*) KPNO No. 1 0.9 m, 200 s.

ciently smooth to permit a deconvolution. A related question is whether the data can be acceptably fitted by seeing-convolved King models. Studies of globular cluster profile fitting have generally neglected seeing effects since determined core radii for most clusters are usually much larger than the seeing disk radius. However, a proper accounting for the effect of seeing is essential when studying clusters that have surface brightness cusps.

We find it convenient to fit our empirical PSFs with an analytic model for use in computing convolutions. Several models for the PSF were considered including single Gaussian, double Gaussian, and Lauer's (1985) Gaussian plus Gaussian-convolved exponential. We find that the latter two models both provide good fits to the range of PSFs obtained at CTIO and KPNO. We adopt the double Gaussian because it leads to a convenient form for the convolution integral.

The double Gaussian PSF model can be written

$$g(r) = \frac{\alpha}{2\pi\sigma_1^2} \exp\left(\frac{-r^2}{2\sigma_1^2}\right) + \frac{1-\alpha}{2\pi\sigma_2^2} \exp\left(\frac{-r^2}{2\sigma_2^2}\right), \quad (1)$$

where $0 < \alpha < 1$, and $\sigma_1 \leq \sigma_2$. The narrower Gaussian ($\sigma_1 \sim 0''.6$) represents the core of the PSF, while the broader Gaussian ($\sigma_2 \sim 1''$) represents the wings. It is straightforward to show that the two-dimensional convolution of an axisymmetric cluster profile model $f(r)$ with the PSF function $g(r)$ is given by

$$f*g(r) = \frac{\alpha}{\sigma_1^2} \exp\left(\frac{-r^2}{2\sigma_1^2}\right) \int_0^\infty dr'r' \exp\left(\frac{-r'^2}{2\sigma_1^2}\right) I_0\left(\frac{rr'}{\sigma_1^2}\right) f(r')$$
$$+ \frac{1-\alpha}{\sigma_2^2} \exp\left(\frac{-r^2}{2\sigma_2^2}\right) \int_0^\infty dr'r' \exp\left(\frac{-r'^2}{2\sigma_2^2}\right) I_0\left(\frac{rr'}{\sigma_2^2}\right) f(r'), \quad (2)$$

where I_0 is the modified Bessel function of the first type of order zero. We compute these convolution integrals numerically for power-law and King model cluster profiles.

Standard χ^2 minimization procedures are used to fit the seeing-convolved models to the data. For the power-law model, both the normalization and the slope are varied. King model fitting is done in two different ways. First, all three parameters of the King model—central surface brightness f_0, core radius r_c, and central concentration $C \equiv \log(r_t/r_c)$ where r_t is the tidal radius—are permitted to vary continuously. Second, we fix the cluster tidal radius at the nominal value and allow the central surface brightness and core radius to vary. The motivation for this second approach is the observation that the central concentration parameter is often not well constrained using data from the central region only.

We find it useful to regard the family of King models as a function of two variables, radius r and central concentration C, for given values of central surface brightness f_0 and core radius r_c

$$f_K(r, C) = f_0 F\left(\frac{r}{r_c}, C\right). \quad (3)$$

Here F is a bivariate function that need be computed only once for a grid of values of r/r_c and C. In carrying out the χ^2 minimization fits, we use bicubic spline interpolation in this grid to determine F for arbitrary values of r/r_c and C.

IV. RESULTS

a) Centering

Data from a $0'.5 \times 0'.5$ square region about the visual center of each cluster were used for the autocorrelation procedure.

TABLE 2

U-BAND SURFACE BRIGHTNESS PROFILES[a]

NGC 6388			NGC 6624			M15		
r (″)	S_U	σS_U	r (″)	S_U	σS_U	r (″)	S_U	σS_U
0.49	9273.	105.	0.49	17860.	1030.	0.40	8483.	126.
0.83	9370.	336.	0.83	14120.	216.	0.68	7925.	288.
1.29	9373.	212.	1.03	14290.	1360.	0.84	7274.	229.
1.61	8991.	216.	1.29	11890.	1130.	1.05	6489.	122.
2.01	8667.	204.	1.61	10470.	745.	1.31	6179.	242.
2.50	7880.	133.	2.01	7557.	495.	1.63	5264.	179.
3.12	7093.	151.	2.50	6593.	519.	2.04	4522.	178.
3.89	6597.	219.	3.12	5709.	356.	2.54	3871.	158.
4.85	5764.	194.	3.89	4824.	307.	3.17	3375.	180.
6.05	5108.	115.	4.85	4021.	351.	3.95	3011.	160.
7.55	4464.	149.	6.05	3432.	208.	4.92	2512.	122.
9.41	3709.	182.	7.55	2705.	185.	6.14	2242.	184.
11.7	2679.	49.	9.41	1869.	123.	7.66	1864.	106.
14.6	2004.	37.	11.7	1403.	53.	9.55	1523.	78.
18.3	1494.	45.	14.6	1266.	39.	11.9	1093.	34.
22.8	1026.	45.	18.3	919.	53.	14.8	957.	54.
28.4	692.	17.	22.8	698.	32.	18.5	716.	31.
35.4	445.	8.3	28.4	498.	12.	23.1	506.	9.9
44.1	273.	7.1	35.4	321.	13.	28.8	426.	38.
55.0	195.	17.	44.1	229.	11.	35.9	280.	12.
68.6	120.	11.	55.0	156.	8.5	44.8	187.	12.
85.6	75.	2.4	68.6	108.	5.6	55.8	119.	8.8
107.	54.	4.2	85.6	79.	8.9	69.6	77.	3.3
133.	25.	2.4	107.	84.	31.	86.8	51.	2.5
			133.	60.	15.	108.	41.	8.5

[a] See Fig. 1 for description of intensity units.

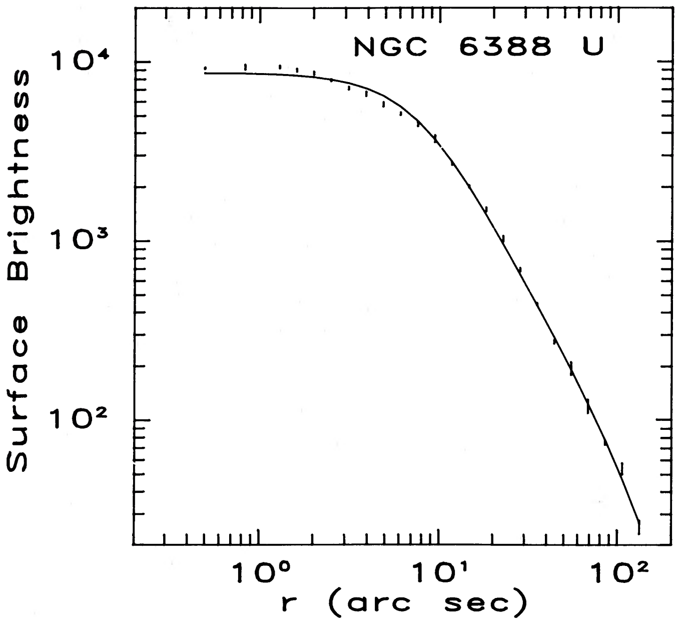

FIG. 2*a*

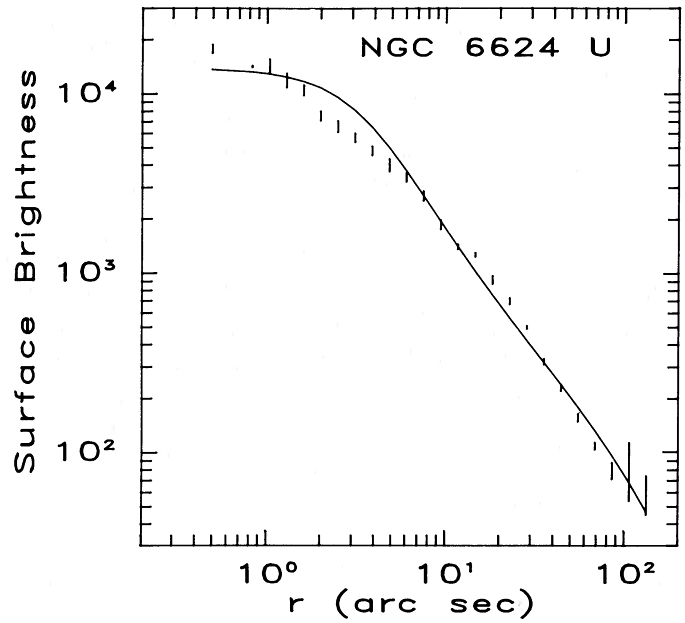

FIG. 2*b*

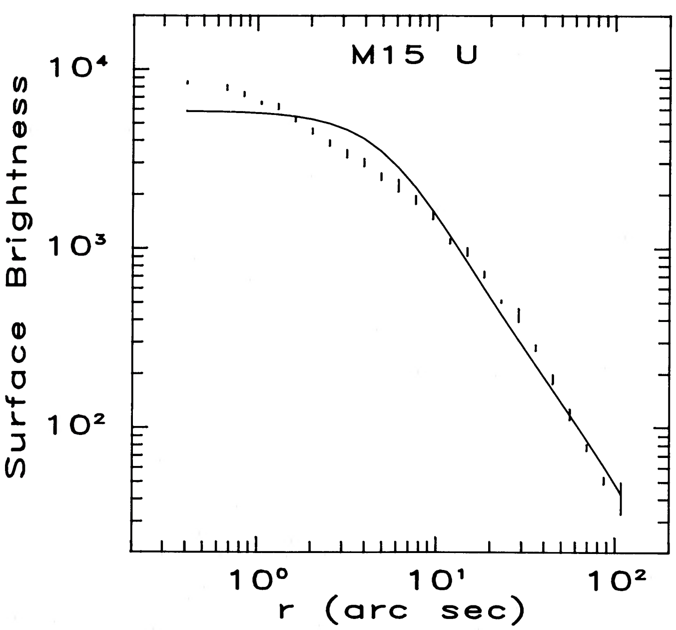

FIG. 2*c*

FIG. 2.—King model fits to the entire surface brightness profiles of (*a*) NGC 6388, (*b*) NGC 6624, and (*c*) M15. While the seeing-convolved King model fit to NGC 6388 has a relatively large χ^2/ndf value, 5.2, it tracks the profile quite well. The seeing-convolved King model fits to NGC 6624 and M15 are unacceptable based on their failure to track the behavior of the inner parts of the profiles and their very large χ^2/ndf values, 14 and 24, respectively.

Varying the length of the side of the centering region from 0'.125 to 1'.0 produced changes of no more than 0".5 in the determined locations of the cluster centers. To provide another test of the reproducibility of the determined centers, we redetermined the centers using the maximum symmetry algorithm developed by Hertz and Grindlay (1985). The agreement was always better than 0".5 between the autocorrelation and maximum symmetry methods. The autocorrelation centers of NGC 6624 and M15 are within 0".5 of the peaks of the central surface brightness distributions.

b) *Surface Brightness Profiles*

Figures 1*a*–*c* illustrate the surface brightness profiles of the three clusters in *U*, and Figure 1*d* illustrates the *R*-band profile of M15. The *U*-band profiles are also presented numerically in Table 2. The advantage of working in the *U* band is clearly demonstrated by a comparison of the error bar sizes in Figures 1*c* and 1*d*. As we have previously noted (Lugger, Cohn, and Grindlay 1985), the surface brightness profiles of NGC 6624 and M15 are similar. Both observed profiles can be approximated by two power laws: one extending from 1" to 10", and the other from 10" to 100". There is a flattening of the profiles inside of a radius of about 1"; our profile model fitting discussed below indicates that this flattening is consistent with being entirely due to seeing. In contrast to these two profiles, the profile of NGC 6388 resembles a King model, flattening out inside a radius of about 2" which is substantially larger than the 0".8 half-power radius of the seeing disk; we show below that this central flattening is not due to seeing.

c) Model Fits

Seeing profiles were determined for the three selected U-band frames by the procedure described above. About five stars were analyzed per frame; the one with the smoothest profile was used to define the PSF. The double Gaussian model gave a good fit in all cases. The determined stellar profile FWHM values for NGC 6388, NGC 6624, and M15 are 1″6, 1″4, and 1″5, respectively.

We first attempted to fit our entire observed profiles of the three clusters with seeing-convolved King models, both with varying and fixed r_t as discussed in § III*c*. A reasonable fit was obtained for NGC 6388 as can be seen in Figure 2*a*; the best-fit parameter values are given in Table 3B ($r_{min} = 0$ case). While the value of χ^2/ndf (χ^2 per degree of freedom) for our fit is 5.2, this fairly large value reflects the small size of the error bars (~2% in the core) rather than indicating a gross divergence between the data and the model. NGC 6388 has a much smoother appearance on the sky than most of the clusters in our sample (including NGC 6624 and M15) and thus its surface brightness profile is particularly well determined. The overall shape of the determined profile is quite similar to the King model, although the data points are systematically about 2 σ above the fit for $r < 2''5$ and about 2 σ below the fit for $2''5 < r < 7''$. Our best-fit core radius and central concentration values of 8″1 and 1.81 (varying r_t) are in excellent agreement with the values of 8″9 and 1.75 tabulated by Webbink (1985) and due, for this cluster, to Illingworth and Illingworth (1976). Another indication of how well NGC 6388 is described by a King model is that the best-fit values of r_c and C remain nearly constant as increasingly large central portions of the profile (up to 20″ radius) are excluded from the fit (see Table 3B).

TABLE 3A

POWER-LAW FITS

r_{max}	NGC 6388 $\frac{d \ln S}{d \ln r}$	NGC 6388 $\frac{\chi^2}{ndf}$	NGC 6624 $\frac{d \ln S}{d \ln r}$	NGC 6624 $\frac{\chi^2}{ndf}$	M15 $\frac{d \ln S}{d \ln r}$	M15 $\frac{\chi^2}{ndf}$
5″..........	−0.32	2.9	−0.72	0.6	−0.62	0.4
7″..........	−0.36	4.6	−0.72	0.6	−0.62	0.4
10″..........	−0.40	6.2	−0.77	1.9	−0.64	0.5
14″..........	−0.53	27	−0.83	4.6	−0.69	3.3
20″..........	−0.63	51	−0.84	4.6	−0.72	4.5
28″..........	−0.66	61	−0.86	5.9	−0.79	13
40″..........	−0.85	190	−0.93	18	−0.81	16

TABLE 3B

KING MODEL FITS[a]

r_{min}	NGC 6388 r_c	NGC 6388 C	NGC 6388 $\frac{\chi^2}{ndf}$	NGC 6624 $\bar{r}_c$	NGC 6624 C	NGC 6624 $\frac{\chi^2}{ndf}$	M15 r_c	M15 C	M15 $\frac{\chi^2}{ndf}$
0″..........	8″1	1.81	5.2	3″4	2.44	14	5″7	2.26	24
	8″2	1.78	5.1	3″7	2.27	16	5″6	2.35	24
5″..........	9″3	1.74	1.0	11″1	2.06	2.2	12″7	1.88	1.5
	9″3	1.73	1.0	3″0	2.37	4.0	12″2	2.01	1.8
7″..........	9″2	1.74	1.0	12″8	1.97	1.3	13″3	1.85	1.2
	9″3	1.73	1.0	3″2	2.33	3.4	12″7	1.99	1.6
10″..........	9″7	1.72	0.9	14″2	1.89	0.7	15″5	1.75	0.5
	9″8	1.71	0.9	3″6	2.28	2.8	14″4	1.94	1.0
14″..........	9″3	1.73	0.9	12″2	1.96	0.4	15″7	1.74	0.5
	9″3	1.73	0.9	5″1	2.13	0.8	14″3	1.94	1.0
20″..........	9″6	1.73	0.8	10″7	1.97	0.4	21″2	1.49	0.2
	8″9	1.75	0.8	6″8	2.00	0.4	16″3	1.89	0.8

[a] For each value of r_{min} (the inner radius for the King model fit), the upper line gives the result for fits with varying r_t and the lower line gives the result for fits with r_t fixed at the values tabulated by Webbink (1985).

In contrast to the case of NGC 6388, no acceptable King model fits to the *entire* profiles of NGC 6624 and M15 could be obtained; the best fits are shown in Figures 2*b* and 2*c* and the best-fit parameter values are given in Table 3B ($r_{min} = 0$ case). The χ^2/ndf values for these fits are 14 and 24, respectively, which are well beyond the acceptable range. Moreover, the King model fits do not reproduce the rising inner profiles of these clusters.

We next fitted the inner parts of the profiles of all three clusters with seeing-convolved power laws. The outer radius r_{max} of the radial range of the fit was varied from 5″ to 40″. The determined power-law indices and corresponding χ^2/ndf values for these fits are given in Table 3A. As can be seen from these results and Figure 3 which shows the $r_{max} = 10''$ fit to NGC 6388, there is no particularly good power-law fit to the inner region of this cluster. Comparison of Figures 2*a* and 3 indicates that although the formal goodness of fit for the King model and power-law fits is similar, the King model better reproduces the general shape of the inner part of the profile. Based on these results, we conclude that there is no evidence for central power-law structure in the profile of NGC 6388. Instead, the core of this cluster appears to be well resolved in our data.

The results presented in Table 3A indicate that the seeing-convolved power-law model gives a good fit to the central regions of both NGC 6624 and M15 out to a radius of about 10″. Thus the true cores of these clusters are unresolved by our data for which the seeing HWHM values are 0″70 and 0″75, respectively. In order to place upper limits on the sizes of the unresolved cores in NGC 6624 and M15, we fitted the central 10″ of these two clusters with power laws modified to have cores. We considered two forms of modified power law: a Hubble-type core, $S \propto (1 + r/r_c)^{-\alpha}$, and a King-type core, $S \propto [1 + (r/r_c)^2]^{-\alpha/2}$. We convolved these profiles with the PSF for a wide range of values of r_c and fitted them to the data for NGC 6624 and M15. For M15, the best fit ($\chi^2/ndf = 0.5$) was obtained in the limit $r_c \to 0$. The value of χ^2/ndf increases with r_c and becomes large ($\gtrsim 2$) for $r_c \gtrsim 1''$. For NGC 6624, the best fit ($\chi^2/ndf \approx 1$) was obtained for $r_c \approx 0''5$; the fit is somewhat poorer in the limit $r_c \to 0$ ($\chi^2/ndf = 1.9$). The value of χ^2/ndf increases with r_c for $r_c \geq 0''5$, and as for M15, $\chi^2/ndf \gtrsim 2$ for $r_c \gtrsim 1''$. Thus we conclude that the unresolved cores in NGC 6624 and M15 have radii of less than 1″.

Figures 4*a* and 4*b* illustrate the power-law fits to the profiles of NGC 6624 and M15 for $r_{max} = 10''$. The corresponding power-law slopes of −0.77 and −0.64 are significantly flatter than the values of −1.09 and −0.91 reported by Djorgovski and Penner (1985). Their fits were carried out over ranges of 3″–20″ for NGC 6624 and 3″–30″ for M15 (they excluded the data inward of 3″ to account for seeing). As can be seen in Table 3A, our determined power-law slopes do become steeper as r_{max} increases, but not as steep as those found by Djorgovski and Penner (1985). Since the goodness of fit deteriorates significantly as r_{max} increases much beyond 10″, we feel that the value of the slope for $r_{max} \approx 10''$ represents the best estimate of the slope of the central power-law cusp for both NGC 6624 and M15.

After establishing that power laws give good fits to the profiles of NGC 6624 and M15 inward of r_{max} for $r_{max} \lesssim 10''$, we

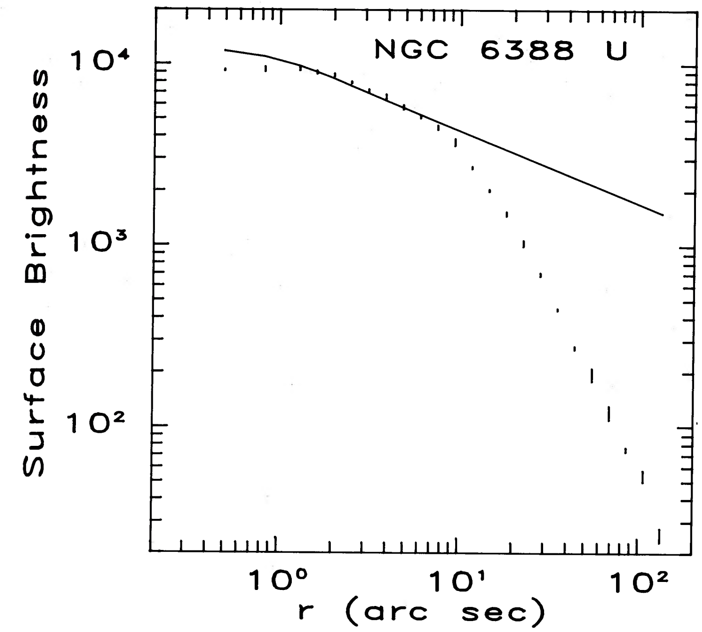

FIG. 3.—Power-law fit to the inner 10″ of the profile of NGC 6388. The poor fit of the seeing-convolved power law indicates that NGC 6388 does not have an unresolved core surrounded by a power-law region.

next fitted the data beyond $r_{\max}$ with a King model. The motivation for this procedure is the prediction by Cohn's (1980) simulations of clusters undergoing core collapse that the outer parts of clusters should continue to resemble King models while power-law cusps develop in the central regions. The results of the King model fits are given in Table 3B where the inner radius of the region fitted by the King model is denoted by $r_{\min}$. For M15 these results do not depend strongly on whether r_t is permitted to vary or is instead fixed at the value of 20'9 tabulated by Webbink (1985). However, for NGC 6624 there is such a dependence, with substantially larger values of r_c obtained when r_t is allowed to vary than when it is fixed at 11'5. As can be seen in Figures 4*a* and 4*b*, King models provide excellent fits to the outer regions ($r_{\min} \geq 10''$) of NGC 6624 and M15 when r_t is allowed to vary; for $r_{\min} = 10''$, the χ^2/ndf values are 0.7 and 0.5, respectively. The corresponding best-fit values of r_c are 14"2 and 15"5, which are about a factor of 3 larger than the values tabulated by Webbink (1985) and due, for these two clusters, to Hertz and Grindlay (1985). This difference is not surprising, since the inner 10″ of the profile is excluded from our fits. When we attempted to fit the entire profiles of NGC 6624 and M15 with King models (Figs. 2*b* and 2*c*), we obtained best-fit r_c values of 3"4 and 5"7, respectively, which are closer to Hertz and Grindlay's (1985) values of 5"2 and 5"5. However, since our fits of simple King models to the entire profiles have unacceptably large χ^2/ndf values, as discussed above, the true core radii of NGC 6624 and M15 should be regarded as indeterminate.

V. DISCUSSION

a) Summary

Our *U*-band CCD surface photometry of the central regions of the clusters NGC 6388, NGC 6624, and M15 allows us to determine high-precision surface brightness profiles. We have carefully analyzed these profiles by fitting seeing-convolved King models and seeing-convolved power laws to assess the evidence for the central surface brightness cusps in NGC 6624 and M15 that have been reported in a number of previous studies reviewed in § I*b*. We chose NGC 6388 as a "normal control" cluster in this study, based on the work of Djorgovski and King (1986).

We find that a King model gives a reasonable fit to the entire profile of NGC 6388. The small size of the surface brightness error bars in the core allows us to detect small but statistically significant systematic deviations of the determined profile relative to the best-fitting King model which describes the overall shape of the profile quite well. Our determined values for the core radius and central concentration of NGC 6388 are in excellent agreement with the previous determination, giving us confidence in our numerical King model fitting algorithm.

Seeing-convolved power-law fits to the central surface brightness profile of NGC 6388 indicate no evidence for a power-law cusp with an unresolved core. The central flattening of the profile of this cluster is thus intrinsic rather than an artifact of seeing. In contrast, the central profiles ($r < 10''$) of both NGC 6624 and M15 are fitted quite well by seeing-convolved power laws. Our analysis places an upper limit of $\sim 1''$ on the unresolved true core radii of these clusters. While this result has been suggested by previous studies, it was not quantitatively demonstrated. The best-fit power-law slopes for the innermost 10″ of the profiles of NGC 6624 and M15 are -0.77 and -0.64, respectively. The outer regions ($r > 10''$) of both NGC 6624 and M15 are well fitted by King models.

b) Interpretation

Simulations of the dynamical evolution of globular clusters have for some time predicted the development of central power-law structure as a result of core collapse. The central surface brightness profiles of NGC 6624 and M15 are in striking agreement with this prediction. Our best-fit power-law slopes are significantly flatter than the value of -1.2 predicted to hold around the time of core collapse in a cluster of identical

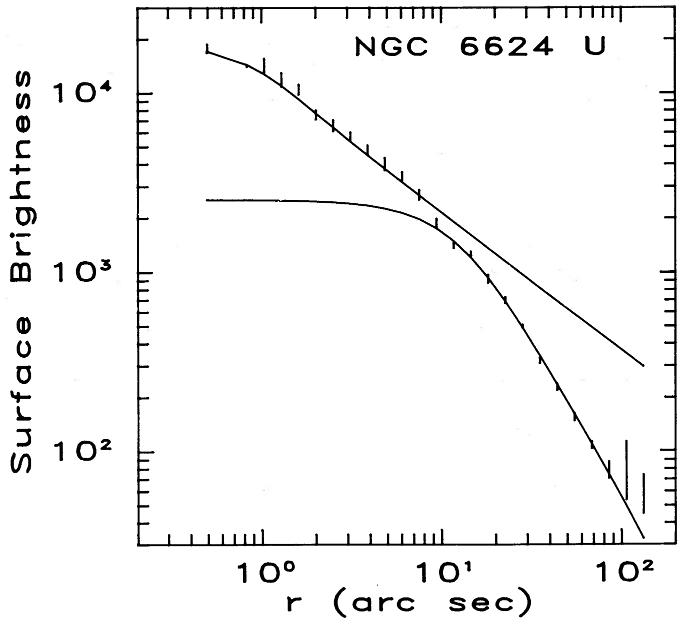

FIG. 4*a*

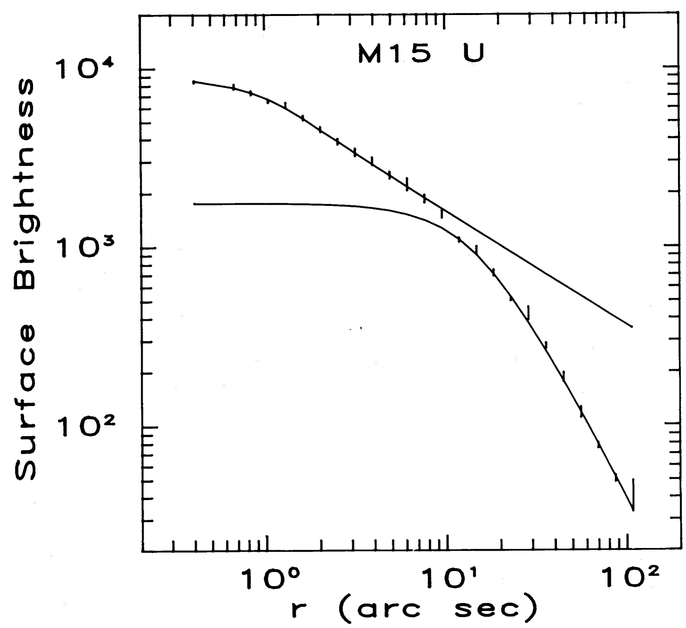

FIG. 4*b*

FIG. 4.—Power-law + King model composite fits to (*a*) NGC 6624 and (*b*) M15. Seeing-convolved power laws are fitted over the range $r < 10''$, while seeing-convolved King models are fitted over the range $r > 10''$. The quantitative measure of goodness of fit provided by χ^2/ndf confirms the good visual impression of the fits. The power-law slopes are -0.77 for NGC 6624 and -0.64 for M15. The core radii for the King models are 14$''$.2 for NGC 6624 and 15$''$.5 for M15.

stars. They are also flatter than the value of -1.0 predicted for a cluster of identical stars undergoing binary-driven postcollapse reexpansion. As discussed in § I*a*, central surface brightness slopes that are significantly flatter than -1 are predicted if the most massive objects in a cluster are nonluminous remnants. Murphy and Cohn (1987) have developed evolving dynamical models for clusters with a realistic mass spectrum undergoing core collapse. These models include up to 15 mass groups covering the main sequence, giants, the horizontal branch, and white dwarfs. The *U*-band surface brightness profile of M15 presented here is well fitted by one of these models (Murphy and Cohn 1987). This model has a red giant mass range of 0.5 $M_\odot$ to 0.8 $M_\odot$, a horizontal branch mass of 0.6 $M_\odot$, and a maximum white dwarf mass of 1.2 $M_\odot$. The relatively steep mass function ($d \ln N/d \ln M = -3.5$) results in a low overall mass fraction of heavy white dwarfs ($<1\%$).

Since the most massive white dwarfs are strongly concentrated toward the cluster center, they are the dominant stellar type within the central 0.1 pc. Inclusion of heavy nonluminous remnants in simulations of clusters undergoing postcollapse expansion also produces central surface brightness cusps of slope flatter than -1.0 (Lee 1987). Thus our determined central surface brightness profile slopes may be taken as evidence for the presence of a centrally concentrated population of massive white dwarfs in NGC 6624 and M15.

The central power-law slopes of the profiles of NGC 6624 and M15 are intriguingly close to the prediction of -0.75 for the slope of the stellar cusp that would form around a massive black hole at the center of a star cluster (Bahcall and Wolf 1976). The motivation for the suggestion by Bahcall and Ostriker (1975) and Silk and Arons (1975) that massive black holes reside at the centers of globular clusters was to explain high-luminosity X-ray emission from globular clusters. There is now strong evidence that the 10 known, high-luminosity globular cluster X-ray sources are neutron star binaries (Grindlay 1981). This evidence does not rule out the possibility of massive central black holes that are unrelated to the cluster X-ray sources. In such a case, it is necessary to explain how the black hole manages to avoid producing observable X-radiation. The lack of resolvable cores in NGC 6624 and M15 would imply central black hole masses in excess of $10^4\ M_\odot$ (Shapiro 1985). Several studies have shown that the expected rate of tidal destruction of cluster stars by a central black hole of this mass is sufficient to fuel a black hole–powered X-ray source of luminosity well in excess of 10^{38} ergs s^{-1} even for a conservative estimate of the accretion efficiency (Shapiro and Marchant 1978; Cohn and Kulsrud 1978). Another complication with the black hole interpretation of the central power-law cusps in NGC 6624 and M15 is that the presence of nonluminous remnants that are more massive than the stars that dominate the surface brightness profile would reduce the slope of the observable stellar cusp around a massive black hole to a value flatter than -0.75 (Bahcall and Wolf 1977). In sum, the present results cannot be taken as strong evidence for the presence of massive black holes in NGC 6624 and M15. The best means of discriminating between a stellar cusp generated by the presence of a massive black hole and one that results from core collapse without a black hole is observation of the stellar velocity dispersion profile in the cusp region (central 10″ radius). The velocity dispersion increases much more rapidly with decreasing radius when a black hole is present ($\Delta v \propto r^{-0.5}$) than in its absence ($\Delta v \propto r^{-0.1}$). Observations of velocity dispersion profiles for the central few arcsec of clusters can be carried out using the Hubble Space Telescope.

We are indebted to S. Djorgovski and Ivan King for making their cluster surface brightness profile determination software available to us and for communicating their results to us in advance of publication. We would like to acknowledge many illuminating conversations with them. We also much appreciate George Jacoby's advice on the KPNO direct CCD system, Mauricio Navarete's assistance with the CTIO PF–CCD system, Tod Lauer's advice on PSF determination, and Steve Kent's assistance with his profile determination software. This work was supported in part by Sigma Xi Grants-in-Aid of Research to P. M. L. and H. C., an Eloise Gerry Grant from Sigma Delta Epsilon to P. M. L., the Goethe Link Fund and NSF grant AST86-13865 at Indiana University, and NSF grant AST84-17846 and NASA contract NAS8-30751 at Harvard University.

REFERENCES

Bahcall, J. N., and Ostriker, J. P. 1975, *Nature*, **256**, 23.
Bahcall, J. N., and Wolf, R. A. 1976, *Ap. J.*, **209**, 214.
———. 1977, *Ap. J.*, **216**, 883.
Cohn, H. 1980, *Ap. J.*, **242**, 765.
———. 1985, in *IAU Symposium 113, Dynamics of Star Clusters*, ed. J. Goodman and P. Hut (Dordrecht: Reidel), p. 161.
Cohn, H., and Hut, P. 1984, *Ap. J. (Letters)*, **277**, L45.
Cohn, H., Hut, P., and Wise, M. 1987, to be submitted to *Ap. J.*
Cohn, H., and Kulsrud, R. M. 1978, *Ap. J.*, **226**, 1087.
Cordoni, J.-P., and Aurière, M. 1981, *Astr. Ap.*, **100**, 307.
Djorgovski, S. 1987, in *IAU Symposium 126, Globular Cluster Systems in Galaxies*, ed. J. E. Grindlay and A. G. D. Philip (Dordrecht: Reidel), in press.
Djorgovski, S., and King, I. R. 1984, *Ap. J. (Letters)*, **277**, L49.
———. 1986, *Ap. J. (Letters)*, **305**, L61.
Djorgovski, S., and Penner, H. 1985, in *IAU Symposium 113, Dynamics of Star Clusters*, ed. J. Goodman and P. Hut (Dordrecht: Reidel), p. 73.
Duncan, M. J., and Shapiro, S. L. 1982, *Ap. J.*, **253**, 921.
Goodman, J. 1983, *Ap. J.*, **270**, 700.
———. 1984, *Ap. J.*, **280**, 298.
Grindlay, J. E. 1981, in *X-ray Astronomy with the Einstein Satellite*, ed. R. Giacconi (Dordrecht: Reidel), p. 79.
———. 1985, in *IAU Symposium 113, Dynamics of Star Clusters*, ed. J. Goodman and P. Hut (Dordrecht: Reidel), p. 43.
Heggie, D. C. 1984, *M.N.R.A.S.*, **206**, 179.
Hénon, M. 1961, *Ann. d'Ap.*, **24**, 369.
Hertz, P., and Grindlay, J. E. 1985, *Ap. J.*, **298**, 95.
Hut, P. 1985, in *IAU Symposium 113, Dynamics of Star Clusters*, ed. J. Goodman and P. Hut (Dordrecht: Reidel), p. 231.
Illingworth, G., and Illingworth, W. 1976, *Ap. J. Suppl.*, **30**, 227.
Inagaki, S., and Lynden-Bell, D. 1983, *M.N.R.A.S.*, **204**, 913.
Inagaki, S., and Saslaw, W. C. 1985, *Ap. J.*, **292**, 339.
King, I. R. 1966*a*, *A.J.*, **71**, 64.
———. 1966*b*, *A.J.*, **71**, 276.
———. 1980, in *Globular Clusters*, ed. D. Hanes and B. Madore (Cambridge: Cambridge University Press), p. 249.
———. 1985, in *IAU Symposium 113, Dynamics of Star Clusters*, ed. J. Goodman and P. Hut (Dordrecht: Reidel), p. 1.
Larson, R. B. 1970, *M.N.R.A.S.*, **150**, 93.
———. 1984, *M.N.R.A.S.*, **210**, 763.
Lauer, T. R. 1985, *Ap. J.*, **292**, 104.
Lee, H. M. 1987, in *IAU Symposium 126, Globular Cluster Systems in Galaxies*, ed. J. E. Grindlay and A. G. D. Philip (Dordrecht: Reidel), in press.
Lightman, A. P. 1982, *Ap. J. (Letters)*, **263**, L19.
Lugger, P. M., Cohn, H., and Grindlay, J. E. 1985, in *IAU Symposium 113, Dynamics of Star Clusters*, ed. J. Goodman and P. Hut (Dordrecht: Reidel), p. 89.
Lynden-Bell, D., and Eggleton, P. P. 1980, *M.N.R.A.S.*, **191**, 483.
McMillan, S. L. W. 1986, *Ap. J.*, **307**, 126.
McMillan, S. L. W., and Lightman, A. P. 1985*a*, *Ap. J.*, **283**, 801.
———. 1985*b*, *Ap. J.*, **283**, 813.
Murphy, B. W., and Cohn, H. 1987, to be submitted to *M.N.R.A.S.*
Newell, B., and O'Neil, E. J. 1978, *Ap. J. Suppl.*, **37**, 7.
Ostriker, J. P. 1985, in *IAU Symposium 113, Dynamics of Star Clusters*, ed. J. Goodman and P. Hut (Dordrecht: Reidel), p. 347.
Peterson, C. J. 1976, *A.J.*, **81**, 617.
Shapiro, S. L. 1985, in *IAU Symposium 113, Dynamics of Star Clusters*, ed. J. Goodman and P. Hut (Dordrecht: Reidel), p. 373.
Shapiro, S. L., and Marchant, A. B. 1978, *Ap. J.*, **225**, 603.

Silk, J., and Arons, J. 1975, *Ap. J.* (*Letters*), **200**, L131.
Spitzer, L. 1985, in *IAU Symposium 113, Dynamics of Star Clusters*, ed. J. Goodman and P. Hut (Dordrecht: Reidel), p. 109.
Statler, T. P., Ostriker, J. P., and Cohn, H. 1987, *Ap. J.*, **316**, 626.
Stodółkiewicz, J. S. 1985, in *IAU Symposium 113, Dynamics of Star Clusters*, ed. J. Goodman and P. Hut (Dordrecht: Reidel), p. 361.
Sugimoto, D., and Bettwieser, E. 1983, *M.N.R.A.S.*, **204**, 19P.
Webbink, R. F. 1985, in *IAU Symposium 113, Dynamics of Star Clusters*, ed. J. Goodman and P. Hut (Dordrecht: Reidel), p. 541.

CHARLES D. BAILYN and JONATHAN E. GRINDLAY: Center for Astrophysics, 60 Garden Street, Cambridge, MA 02138

HALDAN COHN and PHYLLIS M. LUGGER: Department of Astronomy, Indiana University, Swain West 319, Bloomington, IN 47405

PAUL HERTZ: Space Sciences Division, Naval Research Laboratory, Code 4121.5, Washington, DC 20375